Community Assembly and Climate Mismatch in Late Quaternary Eastern North American Pollen Assemblages

Clarke A. Knight,[1,2,*] Jessica L. Blois,[3] Benjamin Blonder,[2] Marc Macias-Fauria,[2] Alejandro Ordonez,[4,5] and Jens-Christian Svenning[5]

1. Department of Environmental Science Policy and Management, University of California, Berkeley, California 94720; 2. School of Geography and the Environment, University of Oxford, Oxford OX1 2JD, United Kingdom; 3. School of Natural Sciences, University of California, Merced, California 95343; 4. School of Biological Sciences, Queen's University Belfast, 97 Lisburn Road, Belfast BT9 7BL, United Kingdom; 5. Section for Ecoinformatics and Biodiversity, Department of Bioscience, Aarhus University, Ny Munkegade 114, Aarhus 8000, Denmark

Submitted January 20, 2019; Accepted August 16, 2019; Electronically published December 13, 2019

Online enhancements: supplemental PDF. *Dryad data:* https://doi.org/10.5061/dryad.c07s28s.

ABSTRACT: Plant community response to climate change ranges from synchronous tracking to strong mismatch. Explaining this variation in climate change response is critical for accurate global change modeling. Here we quantify how closely assemblages track changes in climate (match/mismatch) and how broadly climate niches are spread within assemblages (narrow/broad ecological tolerance, or "filtering") using data for the past 21,000 years for 531 eastern North American fossil pollen assemblages. Although climate matching has been strong over the last 21 millennia, mismatch increased in 30% of assemblages during the rapid climate shifts between 14.5 and 10 ka. Assemblage matching rebounded toward the present day in 10%–20% of assemblages. Climate-assemblage mismatch was greater in tree-dominated and high-latitude assemblages, consistent with persisting populations, slower dispersal rates, and glacial retreat. In contrast, climate matching was greater for assemblages comprising taxa with higher median seed mass. More than half of the assemblages were climatically filtered at any given time, with peak filtering occurring at 8.5 ka for nearly 80% of assemblages. Thus, vegetation assemblages have highly variable rates of climate mismatch and filtering over millennial scales. These climate responses can be partially predicted by species' traits and life histories. These findings help constrain predictions for plant community response to contemporary climate change.

Keywords: macroecology, community ecology, community assembly, paleoecology, climate matching/mismatching.

* Corresponding author; email: clarke.knight@berkeley.edu.

ORCIDs: Knight, https://orcid.org/0000-0003-0002-6959; Blois, https://orcid.org/0000-0003-4048-177X; Blonder, https://orcid.org/0000-0002-5061-2385; Macias-Fauria, https://orcid.org/0000-0002-8438-2223; Ordonez, https://orcid.org/0000-0003-2873-4551; Svenning, https://orcid.org/0000-0002-3415-0862.

Am. Nat. 2020. Vol. 195, pp. 000–000.
DOI: 10.1086/706340

Introduction

Climate is often considered the main driver of assemblage structure across large spatial and temporal scales (Webb 1986; Pearson and Dawson 2003). At shorter timescales, however, species may have differential climate responses (Davis 1984; Webb 1986; Bertrand et al. 2011; Ordonez 2013; Svenning and Sandel 2013), leading to mismatch between the assemblage composition and the climate expectation. Mismatches between assemblage composition and climate may arise from habitat differences, dispersal lags, and species traits or from species interactions that structure communities through time and across space, acting on their own and/or interacting with climate (Ackerly 2003; Ricklefs 2004; Blois et al. 2013*a*; Dalsgaard et al. 2013). Such mismatch is of applied importance because it links to assemblage persistence/survival (Dullinger et al. 2015) and ecological forecasting (Svenning and Sandel 2013; Barnosky et al. 2017). Understanding the mechanisms by which assemblages come in and out of equilibrium with climate and what other factors are important in mediating those dynamics is a central goal.

Contemporary time-series data (e.g., Dornelas et al. 2018) are useful for addressing these questions but are limited by short temporal duration. In contrast, fossil pollen records can provide complementary information about assemblage composition over millennial timescales. Although changes in fossil pollen assemblages are often linked with climate (Grimm et al. 1993; Williams et al. 2002; Yu 2007; Blois et al. 2013*a*), processes like dispersal and species interactions may also determine assemblage dynamics (Ricklefs 2004; Jablonski 2008; Blois et al. 2013*b*; Wisz et al. 2013). For example, megaherbivore decline contributed to

novel plant communities at the end of the Pleistocene (Gill et al. 2009, 2012), and transient associations among tree taxa in Europe (Svenning et al. 2008) and North America (Zhu et al. 2012; Talluto et al. 2017) have been linked to postglacial migrational lags. Mechanisms including site inaccessibility or distance beyond refugia (Svenning et al. 2008; Normand et al. 2011; Nogués-Bravo et al. 2014), competition (Svenning et al. 2014), herbivory (Brown and Vellend 2014), or low seed dispersal (Davis 1984; Normand et al. 2011; Nogués-Bravo et al. 2014) have all been discerned from fossil pollen assemblages. The influence of Native American land-use practices on vegetation composition and structure have been recently described from late Holocene pollen assemblages (Crawford et al. 2015). However, linkages between pattern and process have been limited. There is a need to (1) better understand the role of climate change and other processes in driving assemblage dynamics and to (2) understand how this variation can be predicted over time and space.

Our framework leverages assemblage-level metrics to measure climate (mis)match (λ) and climate filtering (δ) against a regional null model (Blonder et al. 2015; described fully in "Methods" and fig. 1). The regional null model describes assemblages that could have been observed in a local assemblage (but that may or may not be present because of taphonomic/sampling biases or broader-scale biogeographic distributions of clades). If climate is the main factor structuring local assemblages and assemblages respond to it rapidly, the climate niches of taxa observed in the assemblage should be better matched to the local climate than those in the regional null assemblage. Mismatch and filtering are thus defined in terms of observed patterns relative to null expectations.

The climate mismatch (λ) metric addresses assemblage climatic mismatch at local sites. Assemblages showing climate mismatch are composed of taxa with climate niches dissimilar to the local observed climate relative to taxa in the regional pool. This can occur when plants lag in their response to climate change (Bertrand et al. 2011; Svenning and Sandel 2013). In contrast, climate matching occurs when assemblages contain taxa with climate niches close to the local observed climate relative to those in the regional pool.

The climate filtering (δ) metric quantifies how assemblages tend to become composed of taxa with restricted climate niches relative to the taxa in the regional pool (Blonder et al. 2015). Filtered climate niches may reflect the outcome of strong climatic constraints, such as extreme conditions that reduce survival strategies of plants at high latitudes (Swenson and Enquist 2007; Hawkins et al. 2014) or high elevations (Pottier et al. 2012), because fewer taxa with broad climate tolerances are found compared with the regional pool. We define permissiveness as the opposite of filtering, occurring when assemblages contain taxa with broader, more variable climate niches relative to the regional pool. Both λ and δ (summarized in table 1) can be calculated within assemblages across time and relative to past climates.

The ecological meaning of these metrics can be mapped onto community assembly processes: environmental filtering, dispersal limitation, and species interactions (HilleRis-Lambers et al. 2012). The strength of environmental filtering is reflected by δ: assemblage composition either is strongly influenced by climate (climate filtering) or is not (climate permissiveness; sensu Kraft et al. 2014). Dispersal limitation and species interactions can also influence λ. For example, positive λ (mismatch between the assemblage-inferred climate and the local observed climate) could be due to species interactions that lead to exclusion of climatically more suitable taxa or to dispersal limitations relative to the regional pool. Negative λ (climate matching) could be produced by small or absent lags relative to climate change or by species interactions that cluster taxa's niches within climate space. The relationship between λ and δ to different mechanisms is summarized in table 2.

Here we quantify climate matching and filtering in plant assemblages between the Last Glacial Maximum (LGM) and the present in eastern North America (Davis et al. 1975; Delcourt and Delcourt 2004; Williams et al. 2009; Shuman et al. 2009). The period includes both rapid and slow change as well as warming and cooling (Clark et al. 2009). Assemblage data come from pollen records (e.g., Neotoma Paleoecology Database; Williams et al. 2018), while paleoclimate estimates come from general circulation models (e.g., Liu et al. 2009).

We use these data to assess functional trait predictors of climate matching and filtering, from morphology (growth form) and phenology (leaf type) to reproduction (seed mass). These traits are ecologically relevant and may constrain vegetation response to climate. We also consider rate of climate change and distance from ice sheet to determine whether they affect fossil pollen assemblage responses to climate.

We hypothesize that mismatch and filtering varied temporally as climate changed, especially during two periods: the fast-warming Bølling-Allerød (14.7 to 12.9 ka) and cooling Younger Dryas (12.9 to ~11.7 ka). We also predict that mismatch and filtering varied spatially as a result of variation in glaciation histories across the study region. We expect more mismatch and filtering in high-latitude assemblages as a result of melting ice sheets that opened up new landscapes (e.g., Chapin et al. 1994; Svenning and Skov 2007). Likewise, we expect more climate matching in southern nonglaciated sites because of more time for immigration, shorter distances to refugia, and longer time for succession. We also expect that assemblages with higher proportions

of herbaceous flora (not including grasses) will exhibit more climate mismatch because of poorer dispersal ability (e.g., Cain et al. 1998). Similarly, assemblages with a higher proportion of taxa with low seed mass should exhibit more climate matching because of better dispersal ability leading to higher range filling (e.g., Nogués-Bravo et al. [2014] with European trees). Last, we predict that assemblages with a higher proportion of broad-leaved taxa will exhibit more climate matching because of rapid deciduous range expansion (e.g., *Ulmus*, *Acer*, *Quercus*, *Carya*, and *Castanea*) inferred from eastern North American refugia throughout the Holocene (Davis 1983).

Methods

Null Model Analysis

Climate matching (λ) and climate filtering (δ) metrics are calculated using a null model to compare how taxa match their climate relative to expectations from sampling a regional pool (fig. 1*a*, 1*b*). To calculate λ and δ, the framework defines two other metrics that relate inferred "assemblage climate" to "observed climate" (simulated climate in the present study) for a given location and time (fig. 1*c*). First, Δ is the median distance between assemblage-inferred climate (mean climate niche of all taxa in the assemblage, similar to community temperature; e.g., DeVictor et al. 2012) and random samples of niche values from taxa present in the assemblage (allowing for the incorporation of intrataxon niche breadth). Second, Λ is the vector between assemblage-inferred climate and observed climate and indicates differences between the observed climate and the climate that would be inferred on the basis of the presence of these taxa. A null distribution of Δ and Λ is generated by sampling assemblages of equal richness from the regional pool, which comprises taxa that are climatically suitable for the location. Finally, standardized climate deviations (δ and λ) are obtained by comparing observed values of Δ and Λ to those generated under the regional expectation, via z-transformation:

$$\delta = \frac{\Delta_{\text{obs}} - \text{mean}(\Delta_{\text{null}})}{\text{sd}(\Delta_{\text{null}})}, \quad \lambda = \frac{\Lambda_{\text{obs}} - \text{mean}(\Lambda_{\text{null}})}{\text{sd}(\Lambda_{\text{null}})}.$$

Thus, for a given location, assemblage patterns are interpretable in terms of how much mismatch is displayed relative to other possible assemblages that could have occurred. A value of 0 for either statistic means that the assemblage does not differ from the regional expectation given a set of climate conditions, while nonzero values indicate that the local assemblage departs from the regional expectation. The regional pool/null expectation may itself vary over space and time (fig. 1*d*). The regional pool comprises all of the taxa available to colonize a given site and allows for the analysis of large-scale effects (Lessard et al. 2012; Cornell and Harrison 2014).

The definition of the regional pool is important because it will affect estimates of climate matching and filtering (Lessard et al. 2012). Different regional pools can be defined in order to ask different ecological questions and determine the sensitivity of results to the regional pool definition (fig. 2; see below).

Occurrence and Climate Data

We obtained pollen assemblage composition data from Maguire et al. (2016). We used 531 fossil pollen assemblages from eastern North America (comprising 106 taxa) since the LGM 21,000 years ago (21 ka). We chose the eastern North America subset of the global Neotoma Paleoecology Database (Williams et al. 2018) because (1) it has consistent and updated age models such that comparison of patterns among sites through time is less biased by age model uncertainty (see below) and (2) this region has a high density of lakes with fossil pollen samples.

At each site, count data were identified to at least the genus level, with the exception of two sets of indistinguishable pollen taxa: "*Ostrya*/*Carpinus*" and "*Ambrosia* type" (e.g., pollen grains that were classified as either *Ambrosia* or *Iva*). We omitted pollen taxa determined only to the family level (e.g., Poaceae, Amaranthaceae, and Asteraceae) for several key reasons. Our analyses focus on the degree of climate mismatch and filtering among the set of taxa included in this specific assemblage, not on identifying changes in vegetation structure that would require all possible data, including that only available at the family level. Scaling up to the family level would reduce power and introduce a greater potential for violating assumptions (e.g., family-level data would produce a more biased estimate of the pooled niche than genus-level data). Because the Poaceae family was removed but it is known that grasses should dominate sites in the western region of the data set, our statistics may be biased in these regions. We tested the influence of taxonomic resolution on analyses via two regional pool definitions (full description below).

All chronologies were updated to the IntCal09 calibration curve (Reimer et al. 2009) and then revised and standardized chronologies among sites by Blois et al. (2011). For all pollen samples, the relative abundance of each genus/taxon was calculated relative to the total pollen sum for the genus-level data set (Blois et al. 2011) and then linearly interpolated to estimate the relative abundance of each taxon at 500-year intervals from 21 to 0 ka (to match the climate data). We then applied a taxon- and site-specific variable threshold, corresponding to 5% of the maximum abundance recorded for each pollen type. This method

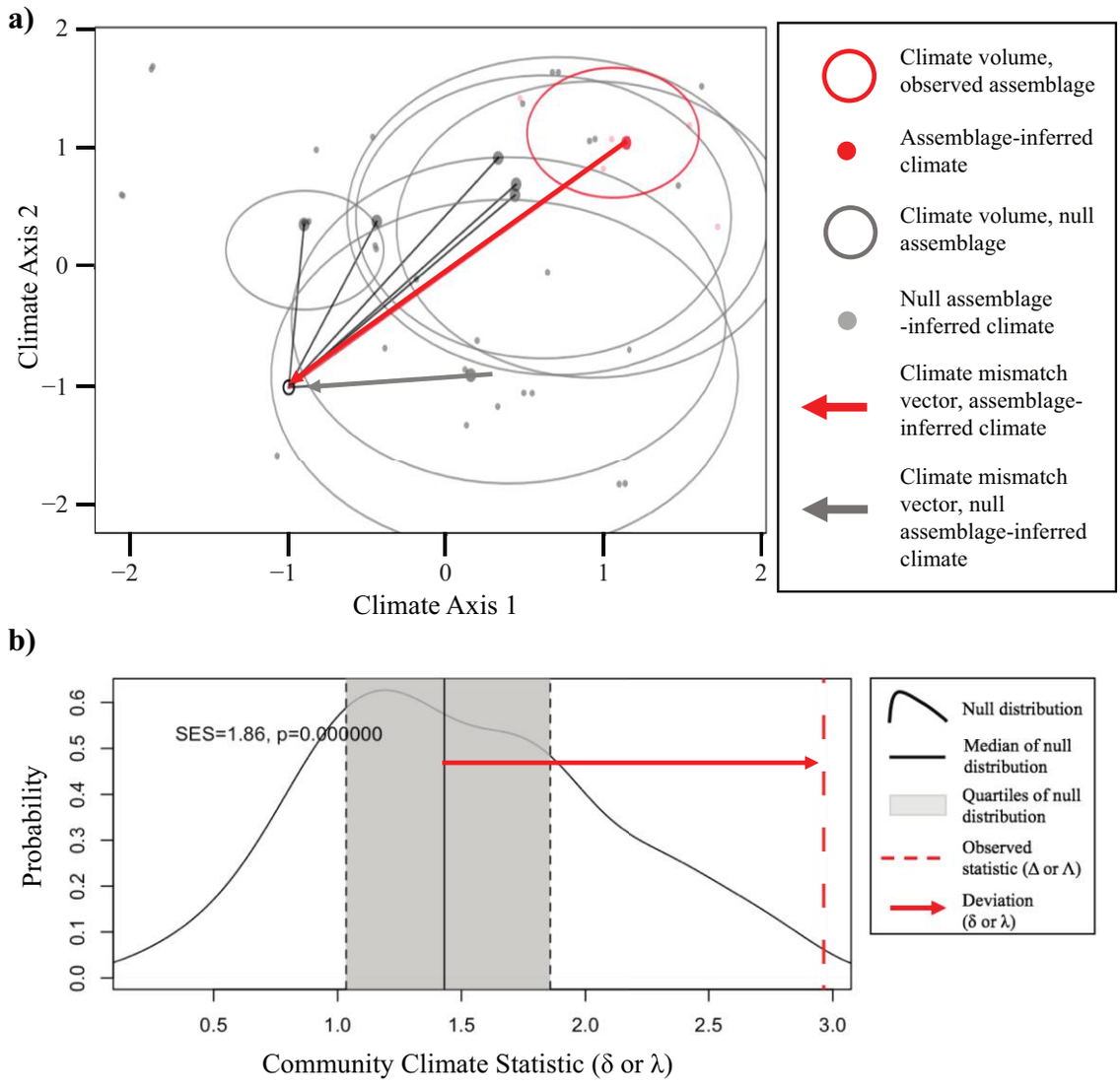

Figure 1: Fundamental community climate concepts are shown in two dimensions (*a*, *b*) for clarity and then over time (*c*, *d*) to illustrate a stylized version of the 21,000-year data set. *a*, Observed assemblage niches are defined by two climate axes. Observed assemblage climate volume (Δ)—the climate space occupied by species in the assemblage at one time, accounting for each species' niche breadth—is indicated (red circle) with the assemblage-inferred climate (red centroid). Climate volume of null assemblages (gray circles; inferred climate as gray centroids) is generated by sampling assemblages of equal richness from the regional pool. The arrows represent the vector between the assemblage-inferred (red arrow) or null assemblage–inferred (gray arrows) climate. The assemblage has smaller climate volume (red circle vs. gray circles) and larger climate mismatch (red vector vs. gray vectors) than expected given the regional pool. In this example, small δ and large λ suggest that the assemblage was structured by environmental filtering and environmental disequilibrium. *b*, The null and observed values for λ, along with projections of the mismatch vector, are shown in two dimensions (the same graph could be made for δ). The null distribution (solid black curve) is shown in two dimensions along with the median (solid vertical line), 25% and 75% quantiles (shaded rectangles), and the observed λ value (dashed red line). In this example, λ is significantly larger ($P > .01$) than the null distribution. *c*, Same as *a* but incorporating a time dimension for the same concepts. The observed climate trajectory is shown (black line) with solid squares at four time points. Observed assemblage niches are defined by multiple climate axes at a given time. Observed assemblage climate volume (Δ) is indicated (solid circle) with the community-inferred climate (solid colored square). Climate volume of null assemblages (dashed circles; inferred climate as a cross-hatched square) are generated by sampling assemblages of equal richness from the regional pool. The colored arrows represent the vector between the community-inferred or null assemblage–inferred climate and the observed climate at one time. *d*, Same as *b* but incorporating a time dimension for the same concepts. Climate deviations (δ, climate volume; λ, climate mismatch) are calculated by comparing the null distributions (curves) with the observed statistics (dashed vertical lines) at different time steps. Quartiles (shaded rectangles) and medians (solid vertical line) are depicted. SES = standard effect size.

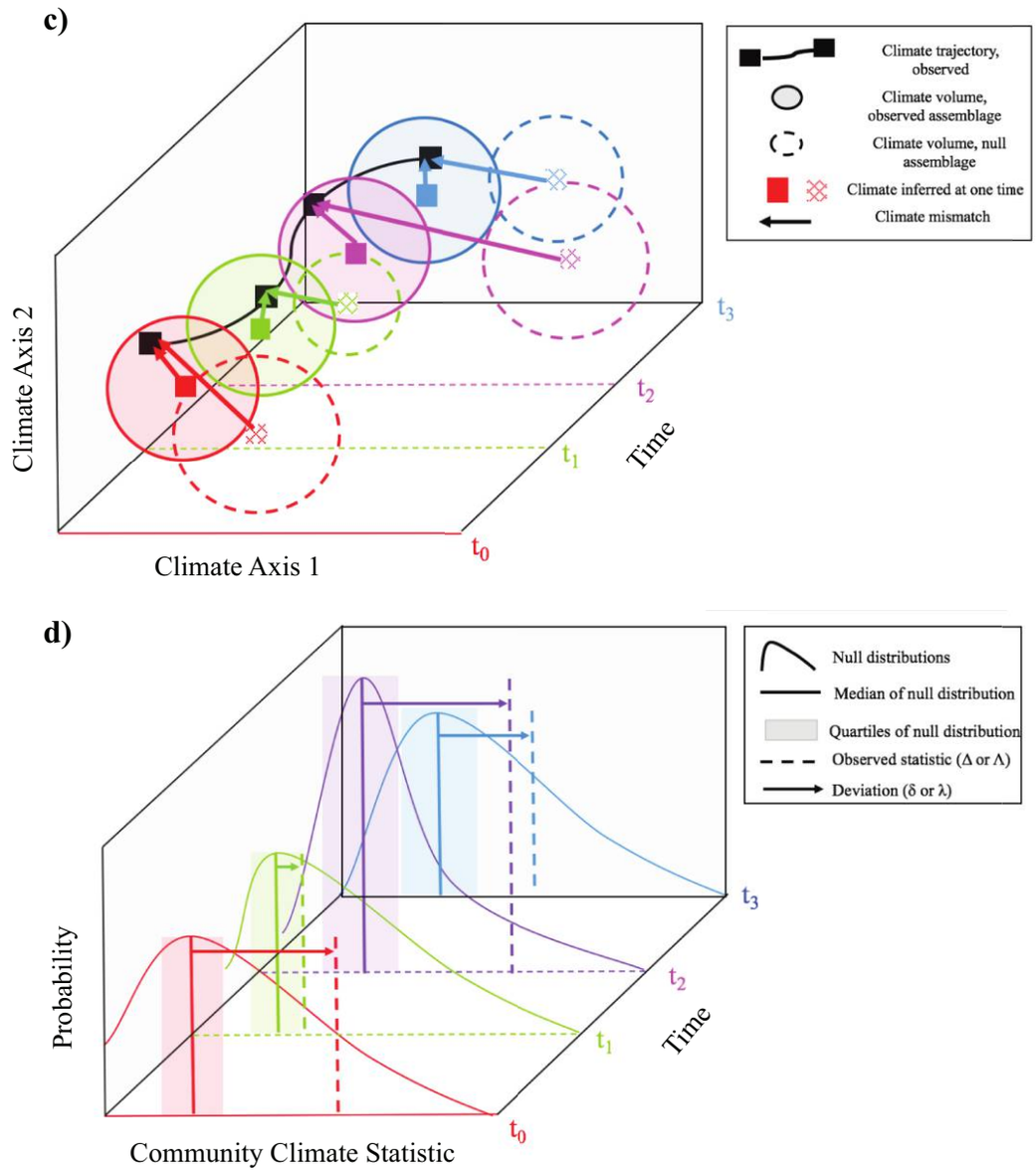

Figure 1 (*Continued*)

most accurately reconstructs turnover compared with modern vegetation based on Forest Inventory and Analysis data relative to five other threshold calculations, effectively downweighting the importance of genera with species that are large pollen producers (Nieto-Lugilde et al. 2015).

Table 1: Climate statistics for positive and negative values of λ and δ, from Blonder et al. (2015)

Metric	Negative values (<0)	Positive values (>0)
λ	Climate matching	Climate mismatching
δ	Climate filtering	Climate permissiveness

We obtained climate data from transient simulation runs using the Community Climate System Model (CCSM3) general circulation model (SynTraCE-21; Liu et al. 2009, 2010), with decadal averages from 22 ka to the present. CCSM3 simulations were debiased and downscaled to a 0.5° × 0.5° resolution, then aggregated to 200-year averages centered on 500-year time slices from 21 to 0 ka (see Lorenz et al. 2016). Mean annual temperature and mean

Table 2: Summary of ecological processes and interpretations of our framework's statistics

Metric	Ecological process	Mechanisms to produce statistic
λ	Climate, dispersal limitation, or species interaction	Mismatch ($\lambda > 0$) could be due to climatically inappropriate taxa persisting (trailing-edge lags) or appropriate taxa failing to colonize (leading-edge lags), species interactions that lead to displacement of climatically more suitable taxa, adaptive niche evolution, priority effects, limited propagule pressure, or competition
		Matching ($\lambda < 0$) could be due to short or nonexistent lags relative to climate change or to species interactions leading to increased niche packing and clustering of taxa's niches within climate space
δ	Climate filtering	Permissiveness ($\delta > 0$) could be due to an assembly being composed of more ecologically generalist taxa or of taxa from multiple biogeographic regions or to an assembly having broad climatic tolerances
		Filtering ($\delta < 0$) could be due to more ecologically specialist taxa, taxa from fewer biogeographic regions, strong climate constraints, or narrow climatic tolerances

annual precipitation were used because they are physiologically relevant (Pearson and Dawson 2003; Van Mantgem and Stephenson 2007; Kosanic et al. 2018) and are accurately reconstructed where validation data are available (Lorenz et al. 2016).

Niche Estimation

Our framework assumes that estimates of taxa's climate niches are unbiased. However, the fundamental niche of a taxon is not accurately represented by the climate space filled at any single time (Jackson and Overpeck 2000). We partially addressed this bias by integrating multiple realized niche estimates from different time bins across 21,000 years of climate-occurrence data, effectively pooling the niche estimates over multiple instances of different realized climates. Such "pooled niches" (Veloz et al. 2012) approximate the fundamental niches and minimize bias caused by estimating niches from climate and occurrence data. We also assumed niche conservatism at millennial timescales, consistent with evidence in plants at the same timescales (Peterson 2011; Lee-Yaw et al. 2016; but see Ackerly 2003; Pearman et al. 2008; Hoffmann and Sgro 2011; Donoghue and Edwards 2014).

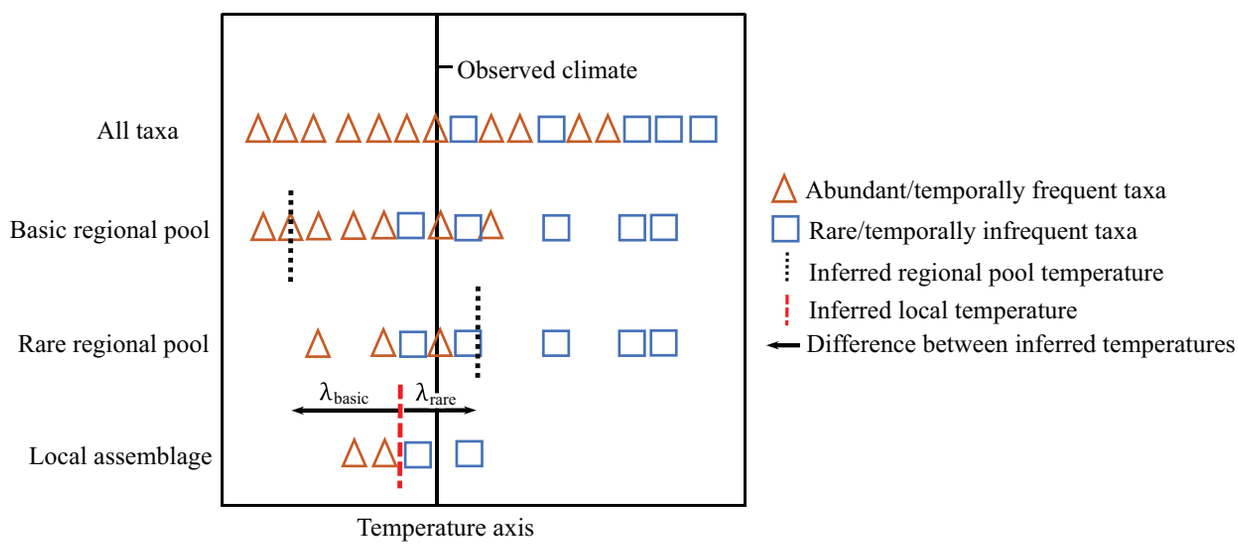

Figure 2: Different regional pool definitions can affect the magnitude and direction of λ and δ statistics. In this example, regional pools are illustrated for a set of taxa along a temperature axis. The basic regional pool contains abundant/temporally frequent taxa (orange triangles) and rare/temporally infrequent taxa (blue squares), and the community-inferred temperature of the regional pool is on the far left of the temperature niche axis (black dotted vertical line). Abundant taxa were removed to form the rare regional pool, which shifted the inferred temperature of the regional pool to the right along the temperature niche axis. The local assemblage has its own inferred temperature (red dashed vertical line). Lambda (λ) is the difference between the inferred regional pool temperature and the inferred local assemblage temperature. In this example, λ values are different depending on whether the local assemblage is compared relative to the basic or rare pool.

Realized climate niches were estimated for each assemblage from the CCSM3 simulations of mean temperature and total precipitation. At each time bin, we matched occurrence data for each fossil pollen taxon with the modeled concurrent climate. Then, to account for uneven sampling over time, we randomly sampled 1,000 times (with replacement) from each distribution and time bin to generate a second pooled sample, although this does not correct for errors of omission. Standardized samples for each time slice were pooled together and used as an approximation of the fundamental climate niche for each taxon (fig. S1; figs. S1–S8 are available online). Because the framework relies on observational data, rare taxa from the pollen record are more subject to violations of the assumption that species' climate niches have been accurately characterized. We tested the influence of rarity through a different definition of the regional pool (see below).

Regional Pool Definitions

We used two regional pools (denoted "basic" and "rare" pools) to ask different ecological questions, address potential biases inherent in fossil pollen data, and determine the sensitivity of results to the regional pool definition.

The basic regional pool for each local fossil pollen assemblage and time was defined as all taxa whose geographic ranges overlapped that site and time plus taxa whose range could have been at the local site, regardless of whether a taxon occurred locally. For the latter "potential" taxa, we used three criteria to account for temporal undersampling, spatial undersampling, and dispersal biases. We corrected for temporal and spatial undersampling of the basic regional pool via range-through sampling (following Wilf and Johnson 2004), a convex hull, and a spatial buffer (see the supplemental PDF for details).

A rare regional pool was created, which varied in its treatment of rare taxa. Like the basic pool, it comprised all taxa with overlapping ranges after accounting for range filling, convex hull, and a spatial buffer. However, we ranked the commonness of taxa at every time slice by number of presences and removed the 20% most common taxa at each time step from each site. This allowed testing whether rare taxa respond differently to climate than the most abundant taxa in each assemblage.

Spatial and Physiological Trait Predictors

We selected five predictors, including time (ka), space (latitude and longitude), growth form (tree, shrub, herb, or climber), seed mass, and leaf shape (broad or needle). Spatially, we defined bands as high latitude (>45°N), midlatitude (40°–45°N), and low latitude (<40°N), following Williams et al. (2009). Seed mass data were obtained from the Royal Botanic Gardens Kew Seed Information Database (2019); genus median seed masses were determined from all species occurring in the study area. *Cyrilla racemiflora* has not been described in the literature, so seed mass was estimated from packets sold from Sheffield's Seed Company (https://sheffields.com/seeds/Cyrilla/racemiflora). Seed masses for *Diervilla*, *Engelhardtia*, and *Koenigia* were not available. Genus leaf shape was obtained from the Global Plant Trait Network (GLOPNET) database (Wright et al. 2004).

Growth form information was obtained from Engemann et al. (2016). Because some genera in the data set (e.g., *Acer*, *Betula*, *Salix*, and *Quercus*) include both tree and shrub growth forms, a categorical genus growth form classification is unfeasible. We compiled the growth form of the relevant species for each genus and weighted each genus as a fraction of tree, shrub, herb, or climber. This was then used to estimate assemblage-scale fractions, that is, proportion of each assemblage with a particular trait at each time (e.g., percentage shrub). We used assemblage-mean traits because the mean often best reflects trait function and its impact on the environment (e.g., Grime 1998; Garnier et al. 2015; Umaña et al. 2017).

Statistical Analyses

Statistics were computed for each site and time using the comclim package (ver. 0.9.4; Blonder 2015) in R (ver. 3.3.1; R Development Core Team 2016). Statistical outputs from comclim (for both basic and rare regional pools) have been deposited in the Dryad Digital Repository (https://doi.org/10.5061/dryad.c07s28s; Knight et al. 2020). To test whether covariates explained matching and filtering patterns, we used mixed models with temporal random effects (lme4 ver. 1.1). Predictors were scaled and centered to enable interpretation as effect sizes. We tested for spatial collinearity among predictor variables, where high collinearity between variables was defined as $r > 0.65$, following Lehmann et al. (1998).

Results

Temporal Patterns

Fossil pollen assemblages exhibited strong variation in climate matching (λ) and climate filtering (δ) over time and space (figs. S3, S4); results presented are based on the basic regional pool except where indicated. Between 50% and 85% of pollen assemblages at any given time showed $\lambda < 0$, consistent with local climate matching at the majority of sites (fig. 3). Climate matching was highest before the Bølling-Allerød, when >80% of assemblages

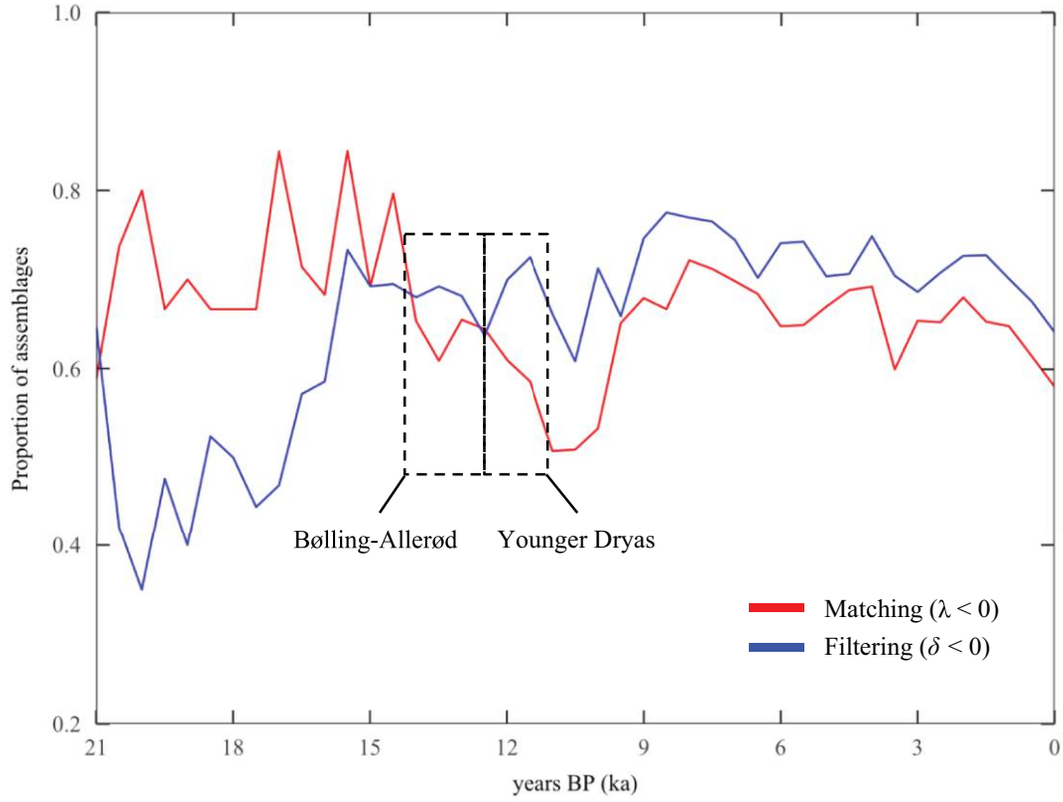

Figure 3: Proportion of assemblages across sites that show matching (red line, $\lambda < 0$) and filtering (blue line, $\delta < 0$) over the past 21,000 years. Across time, the majority of communities matched the local observed climate. Relatively more mismatch and strong filtering from 14.5 to 10 ka were detected, which includes both fast warming during the Bølling-Allerød (14.7 to 12.9 ka) and cooling during the Younger Dryas (12.9 to ~11.7 ka), shown by dashed boxes.

matched climate. The lowest proportion of matching—50% of assemblages—occurred at the end of the Younger Dryas (~11.5 ka), a period of abrupt temperature change; subsequently, assemblage matching rebounded toward the present day in 10%–20% of assemblages. At least half of the δ deviations were negative, corresponding to strong and consistent climatic filtering that strengthened over time. At its peak at 8.5 ka, nearly 80% of assemblages were climatically filtered (fig. 3).

Increased mismatch occurred with rapid climate shifts. We observed fewer assemblages showing climate matching during the Bølling-Allerød and Younger Dryas events (between 14.5 and 10 ka), during which climate shifted rapidly and there were strong changes in the extent of the Laurentide Ice Sheet (fig. 3). No distinct patterns toward permissiveness or filtering relative to rapid climate shifts were found.

Spatial Patterns

Median λ values displayed spatial trends across three latitude bands (high, middle, and low; fig. 4). During deglaciation from 21 to 12 ka, assemblages at the low latitudes (<40°N) and midlatitudes (40°–45°N) generally displayed more climate matching ($\lambda < 0$) than those in the high latitudes (>45°N), which had median λ values closer to zero and indicated weaker climate matching (fig. 4*a*). Immediately after the Younger Dryas cooling event, latitudinal gradients in λ changed: midlatitude assemblages transiently displayed the weakest matching pattern. Starting at 8.5 ka, a strong latitudinal gradient in matching was reestablished, with high-latitude sites showing the lowest climate-matching values and low-latitude sites showing the highest. For δ trends, assemblages show strong filtering, particularly in midlatitude assemblages (fig. 4*b*).

Functional Traits

Multiple variables—that is, latitude, longitude, growth form, and seed mass—were significantly associated at the assemblage level with climate mismatch and filtering trends across space and time. For λ, tree-dominated pollen assemblages showed greater climate mismatch than

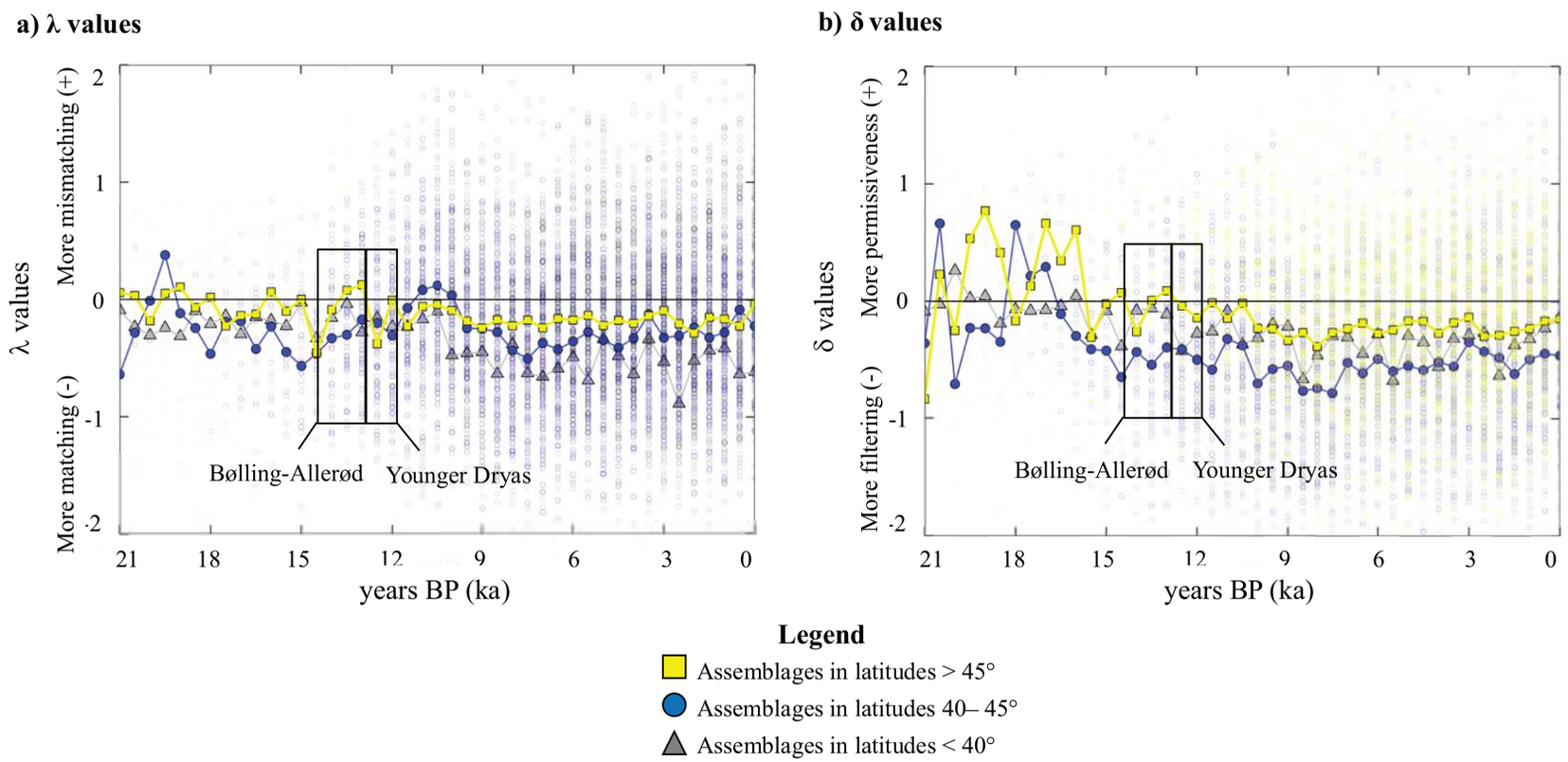

Figure 4: Median λ values (*a*) and median δ values (*b*) plotted by latitudinal bands: high (>45°N; yellow squares), middle (40°–45°N; blue circles), and low (<40°N; gray triangles). For λ, assemblages illustrate spatial trends where high-latitude assemblages exhibit more mismatch relative to lower-latitude assemblages, except at the end of the Younger Dryas event. For δ, assemblages show strong filtering, particularly in midlatitude assemblages.

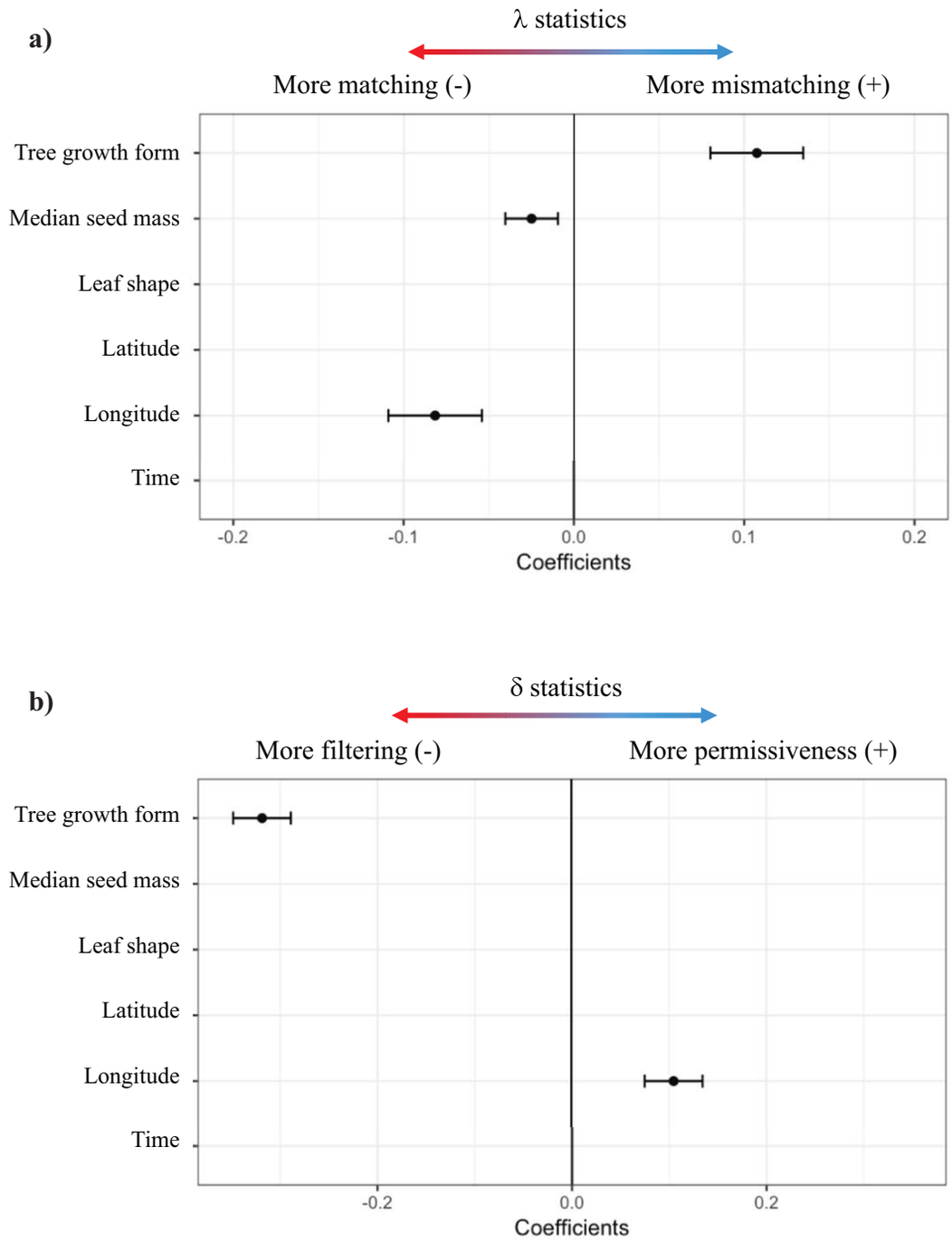

Figure 5: Summary of significant fixed effects from regression models with spatially correlated errors used to predict λ and δ. Negative coefficients correspond to more matching or filtering (red), while positive coefficients correspond to increasing mismatch or permissiveness (blue). Only coefficients significant at the $\alpha = .05$ level are shown.

herbaceous-dominated ones (fig. 5). Assemblages with higher median seed mass were more likely to be matched with climate. Climate mismatch was also found to be more likely at more eastern sites. For δ trends, assemblages with more trees tended to exhibit stronger climate filtering, while those at eastern sites showed more climatic permissiveness (fig. 5). Last, leaf shape was not significantly associated with either metric.

Regional Pool Analysis

We defined two pools (basic and rare) to test whether common taxa dampened assembly signals (rare results are shown in maps in figs. S5S6). Over the past 21,000 years, anywhere from 10% to 30% more assemblages from the basic regional pool displayed climate matching compared with assemblages from the rare pool (fig. S7*a*) except at the end of the Younger Dryas, when the rare pool had 20% more assemblages that matched climate. Results employing the rare regional pool definition showed that climate permissiveness was dominant: up to 90% of assemblages displayed broad ecological tolerances at 19.5 ka, which reduced over time to approximately 70% of assemblages toward the present (fig. S7*b*). Furthermore, median λ values had no discernible latitudinal gradient, and assemblages displayed more climate matching at eastern sites and less in tree-dominated assemblages (fig. S8), but the overall effect of both predictors was weak. Finally, sites with more broad-leaved taxa were associated with stronger climate filtering, and permissiveness was detected at eastern sites and increased over time (fig. S8).

Discussion

We found strong evidence for spatial and temporal variation in climate-driven community assembly, particularly when assemblages lagged behind the climate shifts brought on by the Bølling-Allerød/Younger Dryas interstadial/stadial. High-latitude assemblages exhibited more mismatch, as we hypothesized, as did tree-dominated assemblages consistent with persisting populations and the combination of slower dispersal rates and glacial retreat. Life-history and certain traits were found to be useful predictors of the dynamics of assembly processes. Our findings—that is, assemblages do not always track climate change, and some traits are predictive of mismatch/filtering—showcase the utility of using paleoecological data to address fundamental community assembly questions. The pollen record has shown in the past that proximity to deglaciated areas, the decline of megaherbivores, and biotic interactions are important drivers of assemblage structure and formation (Williams et al. 2009; Gill et al. 2012; Blois et al. 2014). Our findings contribute to a more complete picture not only of the timing and extent of climate mismatch but also of the underlying drivers of assemblage climate mismatch in eastern North America during the late Quaternary.

Climate Matching

Although pollen assemblages predominately matched climate in eastern North America (fig. 3), consistent with climate-matching dynamics dominating (e.g., Webb 1986; Yu 2007; Blarquez and Aleman 2016), different trajectories across time and space were detected within this broad pattern. Temporally, there was a slight trend toward fewer assemblages displaying climate matching through the Holocene (especially during the last two millennia) and a more pronounced excursion toward weaker matching between 14.5 and 10 ka, when rapid climate change occurred (fig. 3). Landscape fragmentation as the Holocene progressed may have been a driver of mismatch. In North America, indigenous populations and their landscape impacts grew from the late Pleistocene to the mid-Holocene, such that forest fragmentation likely occurred (Delcourt and Delcourt 2004). Yet modeled population data (e.g., HYDE 3.1) are poorly resolved in this region and are not fit for application to the long temporal extent of our study; indeed, our results show mismatch increases before the Holocene, when few to no people are known to have inhabited North America. Additional hypotheses for highly localized pre-European agriculture (Muñoz and Gajewski 2010) would suggest a small effect on our results.

Climate-matching trends were spatially structured, as seen in trends across latitude (fig. 4*a*). While assemblages at the majority of sites were matched with local climates, a higher proportion of mismatch was generally observed in the high latitudes (>45°) following glacial retreat (fig. 4*a*), suggesting that assemblage composition did not quickly track local climate. Because λ captures leading and trailing edges of populations, mismatch at northern sites is consistent with many sites being at the leading edge of their ranges, aligning with previous work suggesting that proximity to ice sheets facilitated dispersal into newly deglaciated regions (Svenning and Skov 2004). Weaker climate matching was also detected in the midlatitudes during the early Holocene between 11 and 10 ka (fig. 4*a*), possibly reflecting no-analog associations, which were associated with highly seasonal no-analog climates (Williams et al. 2001) and megafaunal extinctions (Gill et al. 2009). Weaker midlatitude climate matching could also reflect temperate taxa advancement into a previously boreal/arctic region that created a broadened niche space (Davis et al. 1986), which our framework detected as mismatch for boreal/arctic taxa.

Climate Filtering

Broadly, pollen assemblages became more environmentally filtered over time, but there were important spatial distinctions. A higher proportion of sites showed a signal of climatic permissiveness in the eastern part of eastern North America (fig. 4*b*), indicating broader ecological tolerance. The Appalachian Mountains' elevation gradients provide environmental heterogeneity that supported a diversity of taxa, and topographic variability may have

contributed such that greater permissiveness was expressed in areas where local variability in soils or climate is higher.

Traits: Trees and Climate Mismatch

Functional and life-history traits partially explain the climate response of pollen assemblages (fig. 5). Specifically, mismatch was positively related to assemblages that contained a higher proportion of trees and shrubs. These findings agree with long lag times reported for vascular plants from leading-edge lags due to arrival delays to a climatically suitable area and establishment lags dependent on slow growth toward a population carrying capacity (Cain et al. 1998; Svenning et al. 2008). Our study supports the notion of slower tree migration rates compared with herbs, via higher disequilibrium predictions when accounting for growth form. External factors like edaphic conditions (Webb 1986) or landscape structure may have affected tree migration rates, also causing trailing-edge lags, which may be detected as mismatch using this framework.

Seed mass also partially explained assembly dynamics (fig. 5). The hypothesis that low seed mass would be associated with more matching because of better dispersal of light seeds was rejected because, unexpectedly, assemblages with heavier seeds were found to be positively related with climate matching. Dispersal limitations linked to heavier seeds may be offset by animals that eat, transport, and disperse larger seeds over greater distances (Howe and Smallwood 1982). Although seed mass does not indicate the mode of seed dispersal and some large-seeded taxa have low dispersal capacity today (e.g., *Maclura pomifera*), disperser size is correlated in a gradient from anemochory to zoochory (Howe and Smallwood 1982). Genera with the heaviest seed masses (e.g., *Quercus*, *Corylus*, and *Castanea*) are and/or have been dispersed via squirrels, bears, various birds, deer, and now-extinct fauna, all of which may move considerable distances. *Quercus* expanded rapidly during interglacial conditions, and it is thought that birds played a crucial role as dispersal agents (Davis 1983). Additionally, an advantage of large-seeded species is their tolerance to stress (e.g., shade or drought) compared with small-seeded species, which have the advantage of fecundity (Muller-Landau 2010).

Regional Pool Effects

Assemblages defined according to the rare regional pool displayed slightly more climate mismatch, more permissiveness, and divergent trait patterns compared with the basic regional pool definition. Higher climate mismatch and permissiveness in pollen assemblages from the rare pool suggest that rare taxa might have been more tolerant of climate fluctuations or were poorly estimated. In contrast, assemblages represented by the basic regional pool exhibited stronger climatic associations. These findings are consistent with widespread species exhibiting clearer linkages among performance, their environment, and traits than restricted-range species (Umaña et al. 2017).

Methodological Limitations

Our results reflect methodological choices made to minimize the limitations of working with fossil pollen assemblage data and to maximize their potential for understanding community assembly processes. We found important instances of mismatch even though our analyses favored climatic matching in two ways. First, the coarse taxonomic resolution and limited representation of rare taxa biases estimates toward less climate mismatch than studies based on species-level data. Second, compared with other studies (e.g., Svenning and Skov 2004) that consider whole biogeographic regions as potentially occupied by any species, we circumscribed the species pool to a more limited space around a site, reducing the potential for climatic mismatch.

Applying community ecology and trait-based approaches to paleoecological data is inherently challenging given the genus- or family-level taxonomic resolution of most fossil pollen data and that fossil data are not fully interchangeable with contemporary community data (Kullman 1996; Birks and Birks 2008). Furthermore, our methodology assumes niche conservatism at millennial timescales because plants have largely static physiological tolerances at this timescale (Peterson 2011; Lee-Yaw et al. 2016) and at the genus level, although other studies suggest that climate niche evolution is possible (e.g., Ackerly 2003; Pearman et al. 2008; Hoffmann and Sgro 2011; Donoghue and Edwards 2014). Last, our analysis relies on the accuracy of general circulation models (GCMs; Liu et al. 2009). GCM paleoclimate models have large uncertainties but currently provide the best simulations available for key events, for example, the abrupt Bølling-Allerød warming.

Conclusion

We have shown that the ability of fossil pollen assemblages to track climate varies with time, across space, and according to functional and life-history traits. For neoecologists seeking to forecast assemblage persistence/survival under future climate scenarios, our work indicates that traits may predict climate tracking and that patterns from time series can be used to infer assembly processes. By working at the edges of paleoecology and community ecology, our approach provides insight into the prevalence of different community assembly processes over time and increases the mechanistic understanding of past dynamics,

both of which give temporal context to modern concerns in community ecology.

Acknowledgments

We gratefully acknowledge use of the Botanical Information and Ecology Network (BIEN) 3.0 database (B. J. Enquist, B. Boyle, R. Condit, S. Dolins, B. Peet, M. Schildhauer, and B. Thiers), developed with support from the National Center for Ecological Analysis and Synthesis (NCEAS), the iPlant Collaborative, and the US National Science Foundation (NSF) with data (http://bien.nceas.ucsb.edu/bien/biendata/). Support was provided by a Rhodes scholarship (C.A.K.), two Natural Environment Research Council (NERC) independent research fellowships (NE/M019160/1, B.B.; NE/L011859/1, M.M.-F.), and the US NSF (DEB-1257033, J.L.B.). A.O. was supported by a grant (AUFF-F-2018-7-8). J.-C.S. considers this work a contribution to his Villum Investigator project "Biodiversity Dynamics in a Changing World," funded by Villum Fonden (grant 16549), and his Independent Research Fund Denmark/Natural Sciences project TREECHANGE (grant 6108-00078B). We thank the two anonymous reviewers and the managing editor for their constructive feedback.

Literature Cited

Ackerly, D. D. 2003. Community assembly, niche conservatism, and adaptive evolution in changing environments. International Journal of Plant Science 164:S165–S184.

Barnosky, A. D., E. A. Hadley, P. Gonzales, J. Head, P. D. Polly, A. M. Lawing, J. T. Eronen, et al. 2017. Merging paleobiology with conservation biology to guide the future of terrestrial ecosystems. Science 355:eaah4787.

Bertrand, R., J. Lenoir, C. Piedallu, G. Riofrio-Dillon, P. de Ruffray, C. Vidal, J.-C. Pierrat, and J.-C. Gegout. 2011. Changes in plant community composition lag behind climate warming in lowland forests. Nature 479:517–520.

Birks, H. J. B., and H. H. Birks. 2008. Biological responses to rapid climate change at the Younger Dryas–Holocene transition at Kråkenes, western Norway. Holocene 18:19–30.

Blarquez, O., and J. C. Aleman. 2016. Tree biomass reconstruction shows no lag in post-glacial afforestation of eastern Canada. Canadian Journal of Forestry Research 46:485–498.

Blois J. L., N. J. Gotelli, A. K. Behrensmeyer, J. T. Faith, S. K. Lyons, J. W. Williams, K. L. Amatangelo, et al. 2014. A framework for evaluating the influence of climate, dispersal limitation, and biotic interactions using fossil pollen associations across the late Quaternary. Ecography 37:1095–1108.

Blois, J. L., J. W. Williams, M. C. Fitzpatrick, S. Ferrier, S. D. Veloz, F. He, Z. Liu, G. Manion, and B. Otto-Bliesner. 2013*a*. Modeling the climatic drivers of spatial patterns in vegetation composition since the Last Glacial Maximum. Ecography 36:460–473.

Blois, J. L., J. W. Williams, E. C. Grimm, S. T. Jackson, and R. W. Graham. 2011. A methodological framework for assessing and reducing temporal uncertainty in paleovegetation mapping from late-Quaternary pollen records. Quaternary Science Reviews 30: 1926–1939.

Blois, J. L., P. L. Zarnetske, M. C. Fitzpatrick, and S. Finnegan. 2013*b*. Climate change and the past, present, and future of biotic interactions. Science 341:499–504.

Blonder, B. 2015. comclim: community climate statistics package version 0.9.4 for R statistical software (R versions ≥3.0.0).

Blonder, B., D. Nogues-Bravo, M. K. Borregaard, J. C. Donoghue II, P. M. Jørgensen, N. J. B. Kraft, J.-P. Lessard, et al. 2015. Linking environmental filtering and disequilibrium to biogeography with a community climate framework. Ecology 96:972–985.

Brown, C. D., and M. Vellend. 2014. Non-climatic constraints on upper elevational plant range expansion under climate change. Proceedings of the Royal Society B 281:20141779.

Cain, M. L., H. Damman, and A. Muir. 1998. Seed dispersal and the Holocene migration of woodland herbs. Ecological Monographs 68:325–347.

Chapin, F. S., III, L. R. Walker, C. L. Fastie, and L. C. Sharman. 1994. Mechanisms of primary succession following deglaciation at Glacier Bay, Alaska. Ecological Monographs 64:149–175.

Clark, P. U., A. S. Dyke, J. D. Shakun, A. E. Carlson, J. Clark, B. Wohlfarth, J. X. Mitrovica, S. W. Hostetler, and A. M. McCabe. 2009. The Last Glacial Maximum. Science 325:710–714.

Cornell, H. V., and S. P. Harrison. 2014. What are species pools and when they are important? Annual Review of Ecological Systematics 45:45–67.

Crawford, J. N., S. A. Mensing, F. K. Lake, and S. R. H. Zimmerman. 2015. Late Holocene fire and vegetation reconstruction from the western Klamath Mountains, California, USA: a multidisciplinary approach for examining potential human land-use impacts. Holocene 25:1341–1357.

Dalsgaard, B., K. Trojelsgaard, M. González, D. Nogués-Bravo, J. Ollerton, T. Petanidou, B. Sandel, et al. 2013. Historical climate-change influences modularity and nestedness of pollination networks. Ecography 36:1331–1340.

Davis, M. B. 1983. History of deciduous forests of eastern North America and Europe. Annals of the Missouri Botanical Garden 70:550–563.

———. 1984. Climatic instability, time, lags, and community disequilibrium. Pages 269–284 *in* J. Diamond and T. Case, eds. Community ecology. Harper & Row, New York.

Davis, M. B., K. D. Woods, S. L. Webb, and R. P. Futyma. 1986. Dispersal versus climate: expansion of *Fagus* and *Tsuga* into the Upper Great Lakes region. Vegetatio 67:93–103.

Davis, R. B., T. E. Bradstreet, R. Stuckenrath Jr., and H. W. Borns Jr. 1975. Vegetation and associated environments during the past 14,000 years near Moulton Pond, Maine. Quaternary Research 5:435–466.

Delcourt, P. A., and H. R. Delcourt. 2004. Prehistoric Native Americans and ecological change: human ecosystems in eastern North America since the Pleistocene. Cambridge University Press, Cambridge.

DeVictor, V., C. van Swaay, T. Brereton, L. Brotons, D. Chamberlain, J. Heliölä, S. Herrando, et al. 2012. Differences in the climatic debts of birds and butterflies at a continental scale. Nature Climate Change 2:121–124.

Donoghue, M. J., and E. J. Edwards. 2014. Biome shifts and niche evolution in plants. Annual Review of Ecology, Evolution, and Systematics 45:547–572.

Dornelas, M., L. H. Antão, F. Moyes, A. E. Bates, A. E. Magurran, D. Adam, A. A. Akhmetzhanova, et al. 2018. BioTIME: a database

of biodiversity time series for the Anthropocene. Global Ecology and Biogeography 27:760–786.

Dullinger, S., N. Dendoncker, A. Gattringer, M. Leitner, T. Mang, D. Moser, C. A. Mücher, et al. 2015. Modelling the effect of habitat fragmentation on climate-driven migration of European forest understory plants. Diversity and Distributions 21:1375–1387.

Engemann, K., B. Sandel, B. J. Enquist, P. M. Jørgensen, N. Kraft, A. Marcuse-Kubitza, B. McGill, et al. 2016. Patterns and drivers of plant functional group dominance across the Western Hemisphere: a macroecological re-assessment based on a massive botanical dataset. Botanical Journal of the Linnean Society 180:141–160.

Garnier, E., M.-L. Navas, and K. Grigulis. 2015. Plant functional diversity: organism traits, community structure, and ecosystem properties. Oxford University Press, Oxford.

Gill, J. L., J. W. Williams, S. T. Jackson, J. P. Donnelly, and G. C. Schellinger. 2012. Climatic and megaherbivory controls on late-glacial vegetation dynamics: a new, high resolution, multi-proxy record from Silver Lake, Ohio. Quaternary Science Reviews 34:66–80.

Gill, J. L., J. W. Williams, S. T. Jackson, K. B. Lininger, and G. S. Robinson. 2009. Pleistocene megafaunal collapse, novel plant communities, and enhanced fire regimes in North America. Science 326:1100–1103.

Grime, J. P. 1998. Benefits of plant diversity to ecosystems: immediate, filter and founder effects. Journal of Ecology 86:902–910.

Grimm, E. C., G. L. Jacobson, W. A. Watts, B. C. Hansen, and K. A. Maasch. 1993. A 50,000-year record of climate oscillations from Florida and its temporal correlation with the Heinrich events. Science 261:198–200.

Hawkins, B. A., M. Rueda, T. F. Rangel, R. Field, and J. A. F. Diniz-Filho. 2014. Community phylogenetics at the biogeographical scale: cold tolerance, niche conservatism and the structure of North American forests. Journal of Biogeography 41:23–38.

HilleRisLambers, J., P. B. Adler, W. S. Harpole, J. M. Levine, and M. M. Mayfield. 2012. Rethinking community assembly through the lens of coexistence theory. Annual Review of Ecology, Evolution, and Systematics 43:227–248.

Hoffmann, A. A., and C. M. Sgro. 2011. Climate change and evolutionary adaptation. Nature 470:479–485.

Howe, H. F., and J. Smallwood. 1982. Ecology of seed dispersal. Annual Review of Ecology, Evolution, and Systematics 13:201–228.

Jablonski, D. 2008. Biotic interactions and macroevolution: extensions and mismatches across scales and levels. Evolution 62:715–739.

Jackson, S. T., and J. T. Overpeck. 2000. Responses of plant populations and communities to environmental changes of the late Quaternary. Paleobiology 26:194–220.

Knight, C. A., J. L. Blois, B. Blonder, M. Macias-Fauria, A. Ordonez, and J.-C. Svenning. 2020. Data from: Community assembly and climate mismatch in late Quaternary eastern North American pollen assemblages. American Naturalist, Dryad Digital Repository, https://doi.org/10.5061/dryad.c07s28s.

Kosanic, A., K. Anderson, S. Harrison, T. Turkington, and J. Bennie. 2018. Changes in the geographical distribution of plant species and climatic variables on the West Cornwall peninsula (South West UK). PLoS ONE 13:e0191021.

Kraft, N., G. Crutsinger, E. Forrestal, and N. Emery. 2014. Functional trait differences and the outcome of community assembly: an experimental test with vernal pool annual plants. Oikos 123:1391–1399.

Kullman, L. 1996. Norway spruce present in the Scandes Mountains, Sweden at 8000 BP: new light on Holocene tree spread. Global Ecology and Biogeography Letters 5:94–101.

Lee-Yaw, J. A., H. M. Kharouba, M. Bontrager, C. Mahony, A. M. Csergő, A. M. E. Noreen, Q. Li, R. Schuster, and A. L. Angert. 2016. A synthesis of transplant experiments and ecological niche models suggests that range limits are often niche limits. Ecology Letters 19:710–722.

Lehmann, D. R., S. Gupta, and J. Steckel. 1998. Marketing research. Addison-Wesley, Reading, MA.

Lessard, J. P., J. Belmaker, J. A. Myers, J. M. Chase, and C. Rahbek. 2012. Inferring local ecological processes amid species pool influences. Trends in Ecology and Evolution 27:600–607.

Liu, Z., and B. Otto-Bliesner. 2010. Synthesis of transient climate evolution of the last 21-kyr (SynTraCE-21). SynTraCE-21k Workshop, Mount Hood, Oregon, October 10–13, 2010.

Liu, Z., B. L. Otto-Bliesner, F. He, E. C. Brady, R. Tomas, P. U. Clark, A. E. Carlson, et al. 2009. Transient simulation of last deglaciation with a new mechanism for Bølling-Allerød warming. Science 325:310–314.

Lorenz, D. J., D. Nieto-Lugilde, J. L. Blois, M. C. Fitzpatrick, and J. W. Williams. 2016. Downscaled and debiased climate simulations for North America from 21,000 years ago to 2100 AD. Scientific Data 3:160048.

Maguire, K. C., D. Nieto-Lugilde, J. L. Blois, M. C. Fitzpatrick, J. W. Williams, S. Ferrier, and D. J. Lorenz. 2016. Controlled comparison of species- and community-level models across novel climates and communities. Proceedings of the Royal Society B 283:20152817.

Muller-Landau, H. C. 2010. The tolerance-fecundity trade-off and the maintenance of diversity in seed size. Proceedings of the National Academy of Sciences of the USA 107:4242–4247.

Muñoz, S. E., and K. Gajewski. 2010. Distinguishing prehistoric human influence on late-Holocene forests in southern Ontario, Canada. Holocene 20:967–981.

Nieto-Lugilde, D., K. C. Maguire, J. L. Blois, J. W. Williams, and M. C. Fitzpatrick. 2015. Close agreement between pollen-based and forest inventory–based models of vegetation turnover. Global Ecology and Biogeography 24:905–916.

Nogués-Bravo, D., F. Pulido, M. B. Araujo, J. A. F. Diniz-Filho, R. García-Valdés, J. Kollmann, J.-C. Svenning, F. Valladares, and M. A. Zavala. 2014. Phenotypic correlates of potential range size and range filling in European tress. Perspectives in Plant Ecology, Evolution and Systematics 16:219–227.

Normand, S., R. E. Ricklefs, F. Skov, J. Bladt, J. Tackenberg, and J.-C. Svenning. 2011. Postglacial migration supplements climate in determining plant species ranges in Europe. Proceedings of the Royal Society B 278:3644–3653.

Ordonez, A. 2013. Realized climate niche of North American plant taxa lagged behind climate during the end of the Pleistocene. American Journal of Botany 100:1255–1265.

Pearman, P. B., A. Guisan, O. Broennimann, and C. F. Randin. 2008. Niche dynamics in space and time. Trends in Ecology and Evolution 23:149–158.

Pearson, R. G., and T. P. Dawson. 2003. Predicting the impacts of climate change on the distribution of species: are bioclimate envelope models useful? Global Ecology and Biogeography 12:361–371.

Peterson, A. T. 2011. Ecological niche conservatism: a time-structured review of evidence. Journal of Biogeography 38:817–827.

Pottier, J., A. Dubuis, L. Pellissier, L. Maiorano, L. Rossier, C. F. Randin, P. Vittoz, and A. Guisan. 2012. The accuracy of plant

assemblage prediction from species distribution models varies along environmental gradients. Global Ecology and Biogeography 22:52–63.

R Development Core Team. 2016. R: a language and environment for statistical computing. R Foundation for Statistical Computing, Vienna. http://www.r-project.org.

Reimer, P. J., M. G. L. Baillie, E. Bard, A. Bayliss, J. W. Beck, P. G. Blackwell, C. B. Ramsey, et al. 2009. Intcal09 and Marine09 radiocarbon age calibration curves, 0–50,000 years cal BP. Radiocarbon 51:1111–1150.

Ricklefs, R. 2004. A comprehensive framework for global patterns in biodiversity. Ecology Letters 7:1–15.

Royal Botanic Gardens Kew. 2019. Seed Information Database (SID). Version 7.1. http://data.kew.org/sid/ (December 2019).

Shuman, B. N., P. Newby, and J. P. Donnelly. 2009. Abrupt climate change as a catalyst of ecological change in the northeast U.S. throughout the past 15,000 years. Quaternary Science Reviews 28:1693–1709.

Svenning, J.-C., D. Gravel, R. D. Holt, F. M. Schurr, W. Thuiller, T. Münkemüller, K. H. Schiffers, et al. 2014. The influence of interspecific interactions on species range expansion rates. Ecography 37:1198–1209.

Svenning, J.-C., S. Normand, and F. Skov. 2008. Postglacial dispersal limitation of widespread forest plant species in nemoral Europe. Ecography 31:316–326.

Svenning, J.-C., and B. Sandel. 2013. Disequilibrium vegetation dynamics under future climate change. American Journal of Botany 100:1266–1286.

Svenning, J.-C., and F. Skov. 2004. Limited filling of the potential range in European tree species. Ecology Letters 7:565–573.

———. 2007. Could the tree diversity pattern in Europe be generated by postglacial dispersal limitation? Ecology Letters 10:453–460.

Swenson, N. G., and B. J. Enquist. 2007. Ecological and evolutionary determinants of a key plant functional trait: wood density and its community-wide variation across latitude and elevation. American Journal of Botany 94:451–459.

Talluto, M. V., I. Boulangeat, S. Vissault, W. Thuiller, and D. Gravel. 2017. Extinction debt and colonization credit delay range shifts of eastern North American trees. Nature Ecology and Evolution 1:0182.

Umaña, M. N., C. Zhang, M. Cao, L. Lin, and N. G. Swenson. 2017. A core-transient framework for trait-based community ecology: an example from a tropical tree seedling community. Ecology Letters 20:619–628.

Van Mantgem, P. J., and N. L. Stephenson. 2007. Apparent climatically induced increase of tree mortality rates in a temperate forest. Ecology Letters 10:909–916.

Veloz, S. D., J. W. Williams, J. L. Blois, F. He, Z. Otto-Bliesner, and Z. Liu. 2012. No-analog climates and shifting realized niches during the late Quaternary: implications for 21st-century predictions by species distribution models. Global Change Biology 18:1698–1713.

Webb, T. 1986. Is vegetation in equilibrium with climate? how to interpret late-Quaternary pollen data. Vegetatio 67:75–91.

Wilf, P., and K. R. Johnson. 2004. Land plant extinction at the end of the Cretaceous: a quantitative analysis of the North Dakota megafloral record. Paleobiology 30:347–368.

Williams, J. W., E. C. Grimm, J. Blois, D. F. Charles, E. B. Davis, S. J. Goring, R. W. Graham, et al. 2018. The Neotoma Paleoecology Database: a multi-proxy, international community-curated data resource. Quaternary Research 89:156–177.

Williams, J. W., D. M. Post, L. C. Cwynar, A. F. Lotter, and A. J. Levesque. 2002. Rapid and widespread vegetation responses to past climate change in the North Atlantic region. Geology 30:971–974.

Williams, J. W., B. Shuman, and P. J. Bartlein. 2009. Rapid responses of the prairie-forest ecotone to early Holocene aridity in mid-continental North America. Global and Planetary Change 66: 195–207.

Williams, J. W., B. N. Shuman, and T. Webb. 2001. Dissimilarity analyses of late-Quaternary vegetation and climate in eastern North American. Ecology 82:3346–3362.

Wisz, M. S., J. Pottier, W. D. Kissling, L. Pellissier, J. Lenoir, C. F. Damgaard, C. F. Dormann, et al. 2013. The role of biotic interactions in shaping distributions and realised assemblages of species: implications for species distribution modelling. Biological Reviews of the Cambridge Philosophical Society 88:15–30.

Wright, I., P. B. Reich, and M. Westoby. 2004. The worldwide leaf economics spectrum. Nature 428:821–827.

Yu, Z. 2007. Rapid response of forested vegetation to multiple climatic oscillations during the last deglaciation in the northeastern United States. Quaternary Research 67:297–293.

Zhu, K., C. W. Woodall, and J. S. Clark. 2012. Failure to migrate: lack of tree range expansion in response to climate change. Global Change Biology 18:1042–1052.

Associate Editor: Kevin J. Gaston
Editor: Alice A. Winn